Universidad
Carlos III de Madrid

e-Archivo

Institutional Repository

This is a postprint version of the following published document:

Position control of a shape memory alloy actuator using a four-term bilinear PID controller

Álvaro Villoslada [a,*], Naiara Escudero [b], Fernando Martín [a], Antonio Flores [a], Cayetano Rivera [b], Marcelo Collado [b], Luis Moreno [a]

[a] *Carlos III University, Madrid, Spain*
[b] *ARQUIMEA Ingeniería S.L.U., Spain*

Abstract

Shape memory alloy (SMA) actuators have a number of appealing features, such as their low weight or their high force-to-weight ratio, that make them a potential alternative to traditional actuation tech-nologies in fields such as space applications, surgical devices or wearable robotics. In this paper, a type of bilinear controller consisting of a conventional PID controller cascaded with a bilinear compensator, known as BPID, is proposed. Bilinear controllers are a subset of nonlinear controllers, which is why the BPID may be a promising alternative to control the position of a SMA actuator. Nonlinear control tech-niques are commonly applied to control SMA actuators, because of their nonlinear behavior caused by thermal hysteresis. The BPID controller is simpler and easier to implement than other nonlinear control strategies, which makes it a very appealing candidate to control SMA actuators. The performance of the BPID controller has been compared with other two controllers, a conventional PID and a commuted feed-forward PIPD, controlling a real SMA actuator. To this end, a set of five tests has been defined, in which the controlled actuator must follow a series of position references. From these tests, the position and error of the actuator have been plotted, and a series of metrics has been computed to have quantitative mea-surements of the performance of the three controllers. It is shown that, in most of the experiments, the BPID has a better performance than the other two tested controllers, especially tracking step references. However, the power consumption is slightly higher when the actuator is controlled with this strategy, although the difference is minimal. Also, the BPID imposes greater energy variations to the SMA actuator, which might affect its service life. Overall, the BPID controller has proved to be a viable alternative to control SMA actuators.

1. Introduction

Technological development and research in new types of materials and manufacturing methods have led to the appearance of increasingly smaller sensors, embedded control systems, lighter and stronger structures, better energy sources, etc. Some fields of mechatronics where miniaturization and weight reduction are of great importance, such as wearable robotics or space applications, have been benefited from these technological advances, resulting in the development of lighter, smaller and thus, more portable devices. However, actuators, which are a key element of a mechatronic device, have not undergone similar development. Power delivery is one of the most important parameters of an actuator

and the cost of miniaturizing traditional devices such as electric motors, hydraulic or pneumatic actuators is an important reduction in the power they can deliver. Nevertheless, there are some actuators that, despite their small size, can deliver a considerable power. Shape memory alloy (SMA) actuators are within this type of devices.

A SMA is a metallic alloy that can recover its original "memorized" shape after being deformed when heated above its transformation temperature, due to a transition between a martensite phase (low temperature) and an austenite phase (high temperature). The most common of these alloys used for actuation is Nickel–Titanium, or Nitinol. The deformation-recovery cycle of Nitinol can be repeated millions of times, provided that the applied deformations are in the recovery range of the alloy. A SMA actuator uses a SMA element as the transducing material of the actuator: the SMA transducer converts thermal energy into mechanical work. If the SMA element is heated by means of the Joule effect, with a

---
* Corresponding author.
E-mail address: alvaro.villoslada@uc3m.es (Á. Villoslada).

simple circuit that applies an electric current to the SMA actuator, two transduction processes take place. First, electric energy is transformed into thermal energy thanks to the Joule effect. This thermal energy triggers the shape recovery process of the SMA element and the resulting recovery energy is transformed into mechanical work. SMAs have several advantages when used as actuators for mechatronic applications. They are small and lightweight, which allows for a reduction in size, weight and complexity of the devices where they are used. The force-to-weight ratio is very high: a 510 µm diameter Flexinol wire can exert a force in tensile deformation of about 35 N [1]. They can be used as biomimetic actuators: when using SMA wires in tensile deformation, the actuation resulting from the deformation-recovery cycle is similar to the behaviour of a human muscle. Finally, their operation is quiet.

SMA actuators have some limitations that have to be addressed so they can be used as an alternative to traditional actuators in mechatronic applications. When used in the form of a wire in tensile deformation, they produce low strains, typically 2–5% of their length (they can reach 8–10% at the expense of reducing their service life). This implies that in applications where great linear displacements are needed, very long SMA wires have to be used. Another limitation is their low actuation bandwidth: being thermally activated actuators, their actuation speed mainly depends on the cooling time of the SMA element, which is strongly influenced by the process of heat convection from the SMA to the environment. The actuation bandwidth can be improved by passive methods like heat sinks or active methods such as air circulation or liquid cooling. Another well known issue of SMAs, and one of the main research topics within the field of SMA actuators, is their nonlinear behavior, which affects their controllability. The reason for this nonlinear operation is that the temperatures at which the transformation from martensite to austenite takes place are different from the ones of the austenite to martensite transformation, giving rise to thermal hysteresis.

The work presented in this document is part of the STAMAS project[1], which is being currently developed by a consortium of European research centers. The objective of this project is to study the suitability and to bring experience on the SMA based actuation technologies addressing terrestrial applications, to research in new concepts of artificial muscles for biofeedback spacesuits, as an alternative to current technologies. The ultimate goal of the STAMAS project is the development of three different SMA-actuated demonstrators. Two of them are countermeasure devices intended to be used inside a spacecraft: one to exercise the legs in order to mitigate muscle mass and bone loss, and another one to exercise the ankles and improve propioception and balance. The third demonstrator is a motion assistance device intended to be used in extravehicular activities (EVA). It is an exomuscular system designed to release astronauts from part of the exhausting effort required to move the fingers of the hand when using an EVA glove.

In our previous work, a commuted feedforward PIPD feedback control strategy, named PIPD for simplicity, has been implemented to control SMA actuators [2]. With the cited method, three short SMA wires were actuated simultaneously, achieving an accurate tracking of the position reference. Despite the good results obtained with this PIPD controller, the control of SMA actuators can be further improved to reduce the error and overshoot produced by the nonlinear behavior of the material. These effects can largely be overcome by applying nonlinear control techniques.

Bilinear systems are a specific type of nonlinear systems which present some interesting characteristics. The type of equation that defines these systems is simple and similar to a linear one. Bruni et al. defined bilinear systems as a class of "nearly" linear systems [3]. Many different techniques and analytical procedures already applied to linear systems are also valid for bilinear systems. In addition, the nonlinear structure presents some important advantages regarding controllability, optimization and modeling. Bilinear controllers, and especially the one implemented in this work, are a good choice to control nonlinear systems with hysteresis because of their simplicity and ease of implementation, compared with more complex strategies. For the above reasons, a four-term bilinear PID (BPID) controller is proposed in this work to control SMA actuators. To the best of our knowledge, no other groups have applied bilinear compensators to control this type of actuators. The purpose is to control the linear motion of a hanging mass with a SMA linear actuator. Exhaustive experiments have been conducted to test the performance of the control approach proposed in this paper. The good behavior of the BPID controller regarding accuracy and smoothness lets us conclude that it is a suitable alternative to control these type of materials.

The rest of this paper is organized as follows. First, Section 2 contains a brief review of related work, paying attention to the different methods that can be applied to control smart actuators and giving some examples. The control strategies implemented in this work are detailed in Section 3. After that, the experimental setup is introduced in Section 4. In Section 5, the results are presented. The discussion about the experimental results is addressed in Section 6 and, finally, the most relevant conclusions are summarized in Section 7.

2. Related work

Many different strategies can be applied to control nonlinear systems. Nevertheless, not all of them are appropriate for systems with hysteresis. SMA actuators present a nonlinear saturated hysteretic behavior during martensite-austenite and austenite-martensite transformations. This hysteresis cycle can be determined either experimentally or it can be approximately modeled using different methods. Position and force control of SMA actuators are topics that have been widely studied during the last decade. Their nonlinear saturated hysteretic behavior originates steady-state errors and limit cycle problems when conventional controllers are used [4,5].

Different techniques can be implemented to control SMA actuators. The controllers vary from simple linear controllers to more complex nonlinear control approaches. Due to the complex behavior caused by their hysteresis cycle, SMA actuators are mostly controlled using nonlinear methods. The most relevant contributions will be reviewed in the next paragraphs.

Due to the hysteretic nonlinear behavior, simple conventional controllers like proportional controllers are not sufficient to achieve precise position control. In [6], a proportional controller is used in active shape control of a flexible beam. Experimental data have shown that a high gain is required to eliminate the steady-state error, but at the cost of a higher overshoot and actuator saturation. Shameli et al. [7] have used a nonlinear variation of a PID controller referred to as PID-P3 controller. Their simulations showed that for large values of error, the cubic term of the regulator, which is the main difference with respect to a traditional controller, produces great control effort that reduces significantly the settling time. The cubic term vanishes for small values of error and the controller works as a conventional PID controller. This technique has not been validated experimentally.

In Yang et al. [8], a first-order system is used to model the step response of a composite beam with SMA actuators located on its surface. The parameters are experimentally determined and the

---

model is used to tune a controller. To control the response of the hybrid composite beam, two methods are used. One of them is a conventional PID feedback controller and the other one is a feedforward controller. The experimental results have shown a reasonable settling time and high overshoot for the PID controller, and long settling time for the feedforward controller.

Popov et al. [9] have used two PID controllers to control a SMA actuator. The first one is adjusted with Ziegler–Nichols. In the second one, which is called Internal Model Control (IMC), the SMA is modeled as successive series of four transfer functions: a gain, a first order transfer function, a second order transfer function, and a dead time. The time response of the IMC controller is significantly better.

Asua et al. [10] have concluded in their experiments that a PI with anti-windup is the best type of position controller for their SMA actuators.

A particular case of controllers that have been successfully applied to SMA actuators are the Pulse Width Modulation (PWM) controllers. This type of controller differs in how the control action that commands the actuator is generated: they use discrete-time PWM signals as control actions. Therefore, this approach can be combined with linear on nonlinear compensators. PWM controllers have shown to be an effective solution reducing the energy consumption of the actuator. This fact has been demonstrated by some researchers. In [11], a PWM controller was used to control a SMA actuator and results showed a 30% reduction in the energy consumed when compared with a conventional PD controller, while maintaining the same position accuracy. An improved PWM technique called Pulse-Width-Pulse-Frequency (PWPF) modulator was used to modulate a PD controller in [12]. It was found that the PD controller with PWPF modulation consumed 50% less energy than the PD controller without modulation.

In recent years, the experimental results using nonlinear controllers show that (in position control of SMA actuators) it is possible to achieve faster tracking and greater accuracy. The most typical configuration is a combination of feedforward and feedback controllers [13–17]. The main idea of the feedforward controllers consists of using an inverse model of the system to generate the appropriate control input to obtain the desired response. A different option is the optimal controller based on the LQR method adopted by Lee and Mavroidis to control SMA actuators [18]. Another type of nonlinear controllers that have been used to control SMAs are those based on gain scheduling. Gain scheduling control is based on the use of a series of linear controllers whose performance is optimized for different operating points of the plant to be controlled. To switch between the different linear controllers, the gain scheduler monitors one or more observable variables to infer in which operating range is the controlled process. There are some examples of gain scheduling control applied to control the position of SMA actuators, such as the works by Jayender et al. [19,20] or Kilicarslan et al. [21]. Andrianesis et al. [22] implemented a gain-scheduled controller to drive the output of the SMA actuation system of a prosthetic hand.

Different procedures can be followed when addressing the problem of modeling and controlling the behavior of systems with hysteresis. Regarding the techniques applied to SMA actuators, these methods will be divided here into model-based controllers and inverse model controllers. These approaches are not restricted to SMA actuators and are also applied to other smart actuators like piezoelectric, piezoceramic and magnetostrictive.

• Model-based controllers.

The controller is designed based on the equations of the system. Representative models of SMA wires are used. An example of a SMA model is the one-dimensional Brinson constitutive model [23], where the stress is related to the state variables of strain, temperature and martensite volume fraction.

The most important difficulty of this type of controllers is to obtain accurate models. In fact, many aspects of nonlinear actuators are not modeled or highly simplified. Any modeling process requires a model validation previous to the controller design.

Asrafiuon and Jala [24] have used a model-based sliding mode control law with SMA actuators. Their model is obtained by combining the motion equation with the heat convection (constitutive law) and phase transformation (hysteresis) equations of the SMA. The resulting controller is used in a three-link planar robot for position control.

Elahinia and Ahmadian [25,26] have developed a nonlinear model of a 1-DOF rotary arm that is SMA actuated. The nonlinear approach uses three models: the arm nonlinear dynamic model, a SMA phase transformation model and a nonlinear heat convection model. They use two controller designs: a temperature-based controller and a stress-based controller. The temperature-based controller is a variable structure controller while the stress-based one is a sliding mode controller.

• Inverse hysteresis model controllers

The compensator is based on an inverse hysteresis model. In a first step, a hysteresis model is built based on the experimental data of the system. The hysteresis model is designed to minimize the error between the real system and the model. In a second step, an open loop controller in which the inverse operation adjusts the actuator input to compensate the hysteresis of the system is implemented. The previous steps produce a linear relationship between the reference input and the system output [27]. In practice, the inverse model cannot cancel completely all hysteresis nonlinearities in SMA actuators, and some authors use a feedback controller together with the feedforward open loop controller [13]. The use of a feedforward controller can speed up the controlled system response and increase the bandwidth when compared with a PID controller. On the other hand, the PID controller provides better tracking performance at low frequencies [28].

Research in modeling the hysteresis of SMA actuators has been very active in the last two decades. These techniques can be classified into two groups:

- Black box-based controllers: the hysteresis (or more frequently its inverse) is modeled as a black or grey box. They exploit the universal approximation properties of neural networks, fuzzy systems and neuro-fuzzy structures. These methods require a large amount of experimental data.

In Asua et al. [10], an experimentally trained neural network is used to cancel the nonlinearities of a SMA wire. The neural network is trained to learn the inverse hysteresis behavior and, after that, a PI with anti-windup control loop is used. Kumagi et al. [14] have proposed a controller with a feedforward part that uses a neuro-fuzzy inference system and a PD controller. Song et al. [15] have designed a neural network feedforward controller for open loop tracking control of a SMA wire actuator without a position sensor. Their neural network controller is an inverse model of the hysteresis that maps the relationship between the applied voltage and the actuator displacement. In Rezaeeian et al. [16], they are focused on the application of an ANFIS inverse controller as a feedforward regulator for force control applications of SMA actuators.

- Phenomenological-based controllers: the hysteresis is modeled by phenomenological hysteresis modeling methods. Preisach models, Krasnosel'skii-Pokrovskii models and Prandtl–Ishlinskii models are operator-based models in which the global behavior is defined by the integral of the hysteresis operators over a specified region. Accurate results are obtained by using the inverse of these phenomenological hysteresis models as a feedforward compensator.

Hughes and Wen [29] have used the Preisach inverse model to control a SMA actuator. In Ahn and Kha [30], the inverted numerical Preisach model is integrated in a closed loop PID control system to compensate the hysteresis in SMA actuators. Majima et al. [17] have developed a control system composed of two control loops: a PID feedback control loop and a feedforward loop. The feedforward loop is used to obtain the desired control input corresponding to the desired displacement. This is obtained from a SMA model based on a Preisach hysteresis model. Hysteresis compensation based on the Krasnosel'skii-Pokrovskii hysteresis inverse model can be found in [31]. They use a parameterized discrete inverse Krasnosel'skii-Pokrovskii model to compensate the hysteresis effects. They have implemented a temperature control law (with electrical current as input) and a model reference controller. The main drawback of the temperature-based feedback controller is that it is difficult to measure the disturbed temperature of the SMA actuator in an open environment. The position control of smart actuators can also be performed using the Prandtl–Ishlinskii inverse model as a feedforward controller. The advantages of the Prandtl–Ishlinskii model are its lower complexity and the possibility to obtain analytically its inverse. Ru et al. [28] have applied this model to describe the hysteresis and the LMS algorithm to estimate the weights of the major hysteresis loop described by the Prandtl–Ishlinskii operator. The inverse of the identified model is used in an open loop adaptive controller to compensate the hysteresis of a piezoelectric actuator.

3. Control strategies

The control strategies that have been tested in this work to control SMA wires are presented in this section. First, the BPID control approach proposed in this paper is detailed. After that, the PID and PIPD techniques are also reviewed because they will be tested for comparison.

3.1. Bilinear PID control

Bilinear systems can be considered as a specific type of nonlinear systems characterized by the following dynamic equation [32]:

$$\dot{\mathbf{x}}(t) = \mathbf{A}\mathbf{x}(t) + \mathbf{b}u(t) + u(t)\mathbf{N}\mathbf{x}(t), \tag{1}$$

where $\mathbf{x} \in \Re^n$ is the state vector, $u(t)$ is a single input, $\mathbf{A}$ is a $n \times n$ matrix of real values, $\mathbf{b}$ is a $n \times 1$ vector of real values, and $\mathbf{N}$ is a $n \times n$ matrix of real constants that contains the nonlinear coefficients.

This class of systems presents interesting properties. The type of nonlinearity shown in Eq. (1) is simple and close to a linear system. This fact allows the application of many techniques and analytical procedures already set up for linear systems. Besides, the nonlinear structure offers other important features.

When the controllability is analyzed, the input controls the state evolution not only additively by means of the term $\mathbf{b}u(t)$, but also in a multiplicative way by means of the term $u(t)\mathbf{N}\mathbf{x}(t)$. This combination of control approaches can result in a more effective control action in some cases. For example, some researchers have concluded that a linear system with input amplitude constraints is, in general, not controllable. This system can be controlled by adding a multiplicative control law [32,33].

When the objective is to model a process, it will be possible to examine those systems where the dynamics depends on the product of the states by the input. This situation happens in some natural or artificial phenomena. For example, a bilinear model can be used to study the basic law of mass action in chemistry. In this system, the reaction rate is proportional to the concentration of reactors with a coefficient given by the catalyst concentration. Mohler has proposed different bilinear models for biochemical and physiological systems [32]. Other examples where bilinear systems can be applied are some economical processes and the electrical power production.

A PID control loop with a bilinear compensator is proposed in this work to control SMA actuators. The BPID control system is essentially a combination of a standard linear PID controller cascaded with a bilinear compensator. To the best of our knowledge, this is the first time that this type of controllers is applied to control SMA actuators. The addition of a bilinear compensator can result in a certain linearization of a nonlinear plant. From a controller point of view, a tuned BPID control system is achieved. According to Minihan [34], the overall performance of the controlled system is improved when a BPID controller is tuned with a minimum knowledge of the plant.

The bilinear controller follows the structure proposed by Martineau et al. [35]. The structure of their controller relies on another advantage of this type of systems, which is that the order of the bilinear system is lower than the corresponding linear model. Martineau et al. concluded that the next equation can be successfully applied to model industrial furnace applications:

$$y(k) = -a\ y(k-1) + b\ u(k-1) + \eta\ u(k-1)y(k-1), \tag{2}$$

where $y(k)$ represents the state in the discrete-time domain, which is the output of the plant in this case, $u(k-1)$ is the discrete input at time $k-1$, and a, b, and η are constants.

The application is completely different here, but it will be demonstrated that the same controller can be used for SMA wires. The output or state to be controlled is the position of the SMA actuator. Rearranging the terms, the following equation is obtained:

$$y(k) = -a\ y(k-1) + b\left[1 + \frac{\eta}{b}y(k-1)\right]u(k-1). \tag{3}$$

This type of nonlinear system can be controlled by the state feedback linearization method. This technique is based on the definition of an additional input v. In the case studied here, the system dynamics is linearized if the relation between the original input and new one is:

$$u(k-1) = \frac{1}{1 + K_b y(k-1)}v(k-1), \tag{4}$$

where $K_b = \eta/b$ is the tuning parameter.

By substituting Eq. (4) in Eq. (3), it can be observed that the system dynamics is now linear:

$$y(k) = -a\ y(k-1) + b\ v(k-1). \tag{5}$$

After that, the linearized system can be controlled by a traditional linear technique such as a PID controller.

The last component added to the bilinear compensator is a term to guarantee that the performance is maintained at the tuning point (null compensation at this point). Finally, the formula of the compensator proposed by Martineau et al. and introduced in the bilinear block is

$$\frac{1 + K_b y_{ref}(k)}{1 + K_b y(k-1)}, \tag{6}$$

where $y_{ref}(k)$ is the reference output at which the PID controller was tuned.

As said before, the final structure of the BPID approach is a four-term controller comprising the three-term PID controller (see the formula in Eq. (11)) and an additional bilinear term. This simple architecture is displayed in Fig. 1. The bilinear term of Eq. (6) is introduced in the bilinear compensator block. An anti-windup system has also been included to limit the control action that can be sent to the actuator.

The gains of the BPID controller may be fixed following different ideas. It is possible to use standard commercial packages or
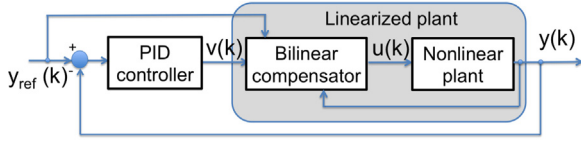
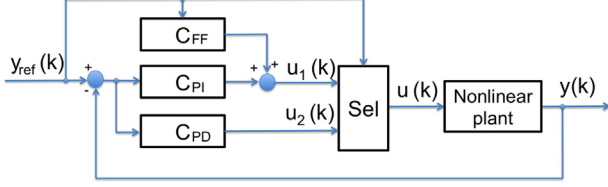**Fig. 1.** BPID control scheme (taken and adapted from [35]).

Fig. 2. PIPD control scheme.

the plant engineer experience. Martineau et al. propose autotuning methods for three-term controllers or least-squares fit to measured plant data [35].

3.2. Commuted feedforward PIPD control

This control strategy, presented in [2], uses a commuting strategy that switches between two controllers: a Proportional-Derivative (PD) controller and a feedforward plus Proportional–Integral (ff+PI) controller. The selection of the controller to be used at each moment is done according to the reference signal to follow. The general idea is to use different controllers for the heating-cooling phase and for maintaining the reference. The output of the controller is converted to a PWM signal that regulates the current flowing through the SMA wire. The controller switches automatically between the PD and the ff+PI controllers depending on its input. If the actuator has to maintain a fixed position given by the input position reference, the PD controller is active. When a new position reference is given to the controller and the actuator has to contract or expand to reach this new position, it switches to feedforward-PI control. The feedforward term of the controller applies a small current to preheat the SMA wire in order to achieve a small contraction. This current is applied only when the SMA actuator contracts from its actual position to a new position given by the input position reference. When the wire expands, the preheating current given by the feedforward term is not applied.

This control architecture is shown in Fig. 2. The PD controller is C_{PD} and the PI regulator is given by C_{PI}. C_{FF} represents the offset introduced by the feedforward component. This approach is ruled by the following formulas and conditions:

$$C_{FF} = \begin{cases} 0; & \text{if } y_{ref}(k) \leq y_{ref}(k-1), \\ u_{FF}; & \text{otherwise}, \end{cases} \quad (7)$$

where i_{FF} is the small current that is added when necessary.

$$C_{PD} = K_{p_{PD}} e(k) + K_{d_{PD}} \frac{e(k) - e(k-1)}{T_s}, \quad (8)$$

where $e(k) = y_{ref}(k) - y(k)$ is the error signal (difference between the position reference and the output), $K_{p_{PD}}$ and $K_{d_{PD}}$ are the gains of the controller, and T_s is the sample time, which is equal to 0.002 s.

$$C_{PI} = K_{p_{PI}} e(k) + K_{i_{PI}} \int_0^k e(\tau) d\tau, \quad (9)$$

where $K_{p_{PI}}$ and $K_{i_{PI}}$ are the gains of the controller.

The selector block (*Sel*) commutes the output of the controller according to the following condition:

$$u(k) = \begin{cases} u_1(k); & \text{if } y_{ref}(k) \neq y_{ref}(k-1), \\ u_2(k); & \text{if } y_{ref}(k) = y_{ref}(k-1). \end{cases} \quad (10)$$

3.3. Conventional PID control

This control strategy is the starting point of the other two tested controllers. The PIPD controller consists of two conventional linear controllers, a PI and a PD, whose output is switched depending on the input position reference, whereas the proposed BPID controller is a conventional PID whose output is multiplied by a bilinear term. For this reason, the performance of a PID will be tested and compared with its two implemented variations.

This method applies the following control reference to assign a value to the current applied to the SMA actuator at each time:

$$current(PWM) = K_p e(k) + K_i \int_0^k e(\tau) d\tau + K_d \frac{e(k) - e(k-1)}{T_s}, \quad (11)$$

where K_p: proportional gain, K_d: derivative gain, K_i: integral gain.

4. Experimental setup

The objective of the performed experiments is to control the linear motion of a hanging mass with a SMA linear actuator. To this end, the proposed BPID controller has been tested along with the other two controllers described in Section 3: a conventional PID controller and a commuted PIPD controller. Their performances have been assessed and compared in terms of accuracy, actuation smoothness and power consumption. The general scheme of the experimental setup is shown in Fig. 3, where the blue lines indicate data connections, the red lines indicate electrical connections and the black lines indicate mechanical connections.

4.1. SMA actuator

The actuator chosen to control the displacement of the hanging mass has been a high-displacement flexible SMA actuator first presented in [36] and refined in [37]. The main field of application of this flexible actuator is wearable robotics, more specifically soft exoskeletons and robotic prostheses, where weight reduction is a major design factor and where large displacements and forces are required. Its main feature is that it is a flexible actuator: it can be bent and still be able to transmit force and motion. This feature allows to overcome one of the limitations of SMA actuators, the limited displacements they can produce, by using a long SMA wire that can be bent to fit the shape of the structure in which the actuator is installed, without limiting the motion of the structure even if it is articulated and changes its shape dynamically. This allows for a better integration and adaptability than other existing high-displacement SMA actuators. The mechanical design of the presented SMA flexible actuator is based on the Bowden cable transmission system, with an approach similar to the designs described in [38] or in [39].

The flexible element of the actuator is a multilayer sheath consisting of a PTFE inner tube to reduce friction losses and a helical stainless steel outer sheath that is rigid enough not to be deformed when the SMA wire contracts, but at the same time it is flexible so the actuator can be bent. The steel outer sheath has another advantageous feature: it acts as a heat sink, increasing the actuation frequency by reducing the cooling time of the SMA element. The SMA transducer is a Flexinol HT wire, with an austenite start temperature of 90 °C, a diameter of 0.5 mm and a pull force of about 35 N [1].
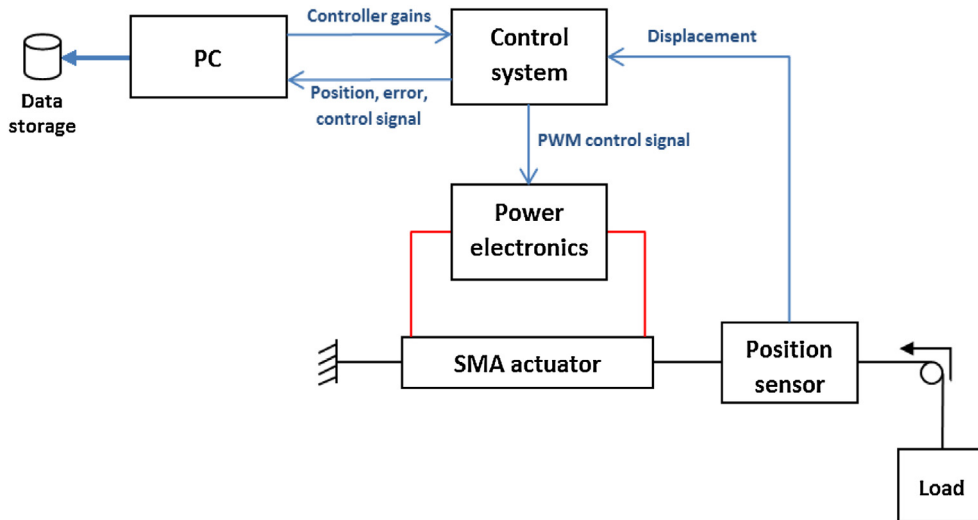
5
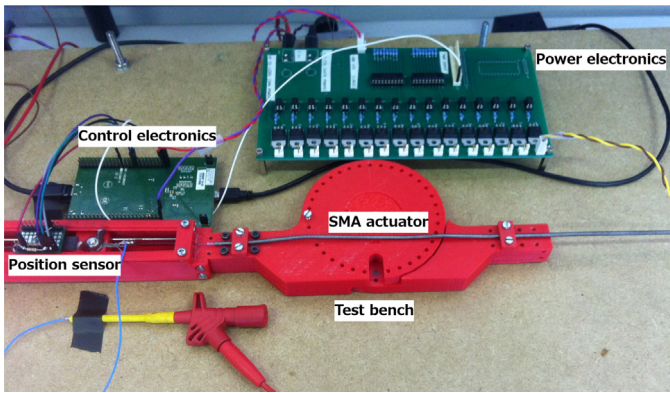
Fig. 3. Experimental setup scheme.

Fig. 4. Test bench.

4.2. Test bench

The described SMA actuator has been installed on a test bench designed to test the effect of the bending angle on the performance of the actuator, although this feature has not been used in the presented control tests and the actuator is installed in a straight configuration. The test bench, shown in Fig. 4, is composed of a rigid structure and the mechanical interfaces to fix the actuator, a linear magnetic position sensor with a resolution of 0.488 μm (AMS AS5311) to measure the contraction of the SMA wire and obtain the position feedback for the control algorithms, the power electronics that provides the electric current to the SMA element, the control and data acquisition electronics and a PC to store the data and communicate with the control electronics.

One end of the SMA wire is fixed to one end of the Bowden sheath, which in turn is fixed to the structure of the test bench. The other end of the Bowden sheath is attached to a part of the test bench containing a movable piece and the position sensor. The non-fixed end of the SMA wire is crimped to the movable piece, which has a magnetic strip on its top side. When the actuator contracts, the movable part is displaced and the position sensor measures the displacement of the magnetic strip. This moving part is attached through one inextensible cord to a load of 40 N, which is the element driven by the SMA actuator in the performed tests and that provides the necessary restoring force to recover the initial length of the SMA wire during the cooling phase.

4.3. Power electronics

As stated before, the most common method to heat a SMA wire and activate its shape memory effect is by the Joule effect, passing an electric current through the wire. To supply this current to the SMA actuator, a 16 channel power driver specially designed to power SMA wires has been used. Each channel consists of a power MOSFET (STMicroelectronics STP310N10F7) commutation circuit driven by a PWM signal from the control electronics [11]. The average value of the output current is directly dependent on the pulse width:

$$\bar{O} = D * O_{Max} + (1 - D) * O_{Min}. \tag{12}$$

Eq. (12) expresses the average value of the output for a PWM signal, where D is the Duty Cycle, O_{Min} is the minimum value of the output and O_{Max} is the maximum value of the output. Each channel of the power electronic hardware is optocoupled from the control unit, providing enhanced security for all connected equipment.

4.4. Control electronics

To design and implement the three tested controllers, as well as to acquire and process all the relevant data to compare their performance, a methodology based on the usage of Rapid Control Prototyping (RCP) software/hardware tools have been used. The used RCP is a custom system developed at Carlos III University of Madrid (UC3M) [40,37]. The UC3M RCP system is based on a powerful and cheap 32 bit microcontroller unit (MCU): the STM32F4 from STMicroelectronics. This MCU runs at 168 MHz, contains a floating point coprocessor and provides plenty Input/Output interfaces. Usually, a RCP system provides a higher level of abstraction than other methods thanks to the usage of graphical programming languages. In the case of the UC3M RCP, the graphical programming language used for the development of the embedded controllers is MATLAB/Simulink, which is well suited and has very powerful toolboxes for the development of control systems. With the UC3M RCP the code generation, compiling and loading into the MCU are completely automatic and transparent to the user.

Each implemented controller consists of two different Simulink block models. The "target" model is compiled and loaded into the control hardware and implements the controller itself, in addition to a series of specific blocks of the STM32F4 MCU peripherals that handle the communication with the position sensor as well as the reception and sending of data from and to the computer.

The second Simulink model is the "host" model and runs on a PC. From this model, the values of the controller gains can be adjusted and sent to the control hardware in real time, while the controller is running. The host model also receives data packets from the MCU containing the position of the actuator measured by the linear position sensor, the error signal measured as the difference between the desired and the real position of the actuator, and the value of the duty cycle of the PWM control signal. This capacity of displaying the real position of the SMA actuator relative to the given reference (which gives a qualitative measurement of the performance of the controller) along with the possibility of adjusting the gains in real time, allows the experimental adjustment of the controller output while it carries out its control task, until the desired performance is achieved. The data received by the host model is stored in PC and can be processed and analyzed to evaluate and compare the performance of the controllers.

5. Results

To evaluate the suitability of the proposed BPID controller in controlling the output position of a SMA actuator, compared with the performance of the other two implemented controllers, a set of five tests has been defined. These tests are intended to show the behavior of the controllers in different situations: performing smooth and continuous motions at different speeds, undergoing small position variations as well as abrupt position changes, and maintaining a fixed position. For each controller, a total of fifteen experiments, three trials for each defined test, have been conducted, consisting of a series of position references that the actuator must follow as accurately as possible.

The following position references have been used to test and compare the performance of the three controllers:

- Sinusoidal reference: three sinusoidal signals with an amplitude of 20 mm peak-to-peak at three different frequencies (0.125 Hz, 0.25 Hz and 0.5 Hz) are applied during 20 s to test the performance of the controllers when following a continuously varying reference at different speeds. For the sake of brevity, only the results of the tests performed with the 0.125 Hz sinusoidal references will be plotted. Numerical results of the tests performed with the three sinusoidal references are summarized in Section 5.4.
- Step reference: two step signals lasting 5 s, with an amplitude of 20 mm and separated by a 30 s interval, are applied to test the behavior of the controlled actuator when it is subjected to a sudden and large position variation and to study its operation in the stationary portion of the reference.
- Incremental step reference: the position reference is increased in steps of 5 mm, from 0 to 20 mm. From this position, the actuator is returned to the starting position in decrements of 5 mm. This test is intended to check the performance of the controlled actuator when it is subjected to small position changes, as well as its stationary behavior at different amplitudes.

The values of the gains of the controllers, adjusted for the completion of the tests described above, are shown in Table 1. These gains have been obtained experimentally by adjusting the values and observing the response of the actuator in real time, thanks to the features of the UC3M RCP.

For each performed test, data provided by the position sensor along with data generated by the RCP system have been stored in different files. In terms of controlling SMA actuators, some parameters are especially important to analyze the performance of an algorithm. Focusing on the most relevant information, the following graphical data will be shown as the results of every experiment, as well as some figures of merit processed from the recorded data:

Table 1
Controller gains.

Strategy	K_p	K_i	K_d	K_b
BPID	0.8	0	0.05	1
Strategy	$K_{p_{PI}}$	$K_{i_{PI}}$	$K_{p_{PD}}$	$K_{d_{PD}}$	u_{FF}
PIPD	0.8	0.25	0.08	0.003	3
Strategy	K_p		K_i		K_d
PID	0.8		0		0.05

- Position – time.
- Error – time.
- Root Mean Squared Error (RMSE).
- Integrated Absolute value of the Error (IAE).
- Mean Absolute Control Signal Increment (MACSI).
- Average power consumption (AVPOW).

5.1. PID

Figs. 5–7 show the results of the PID controller tracking the sinusoidal, step and incremental step references, respectively.

The response of the controller is not bad, taking into account that this is a linear controller driving a nonlinear actuator. The tracking performance during the ascending parts of the reference is good, with only a small overshoot of 0.3 mm and close to the reference. There is a point during the descending parts of the actuation cycle beyond which the actuator is not able to follow the reference, due to the cooling time of the SMA wire.

Regarding the performance of the PID controller tracking a step reference (Fig. 6), a surprisingly good behavior is observed again. The response of the controller is fast (it takes 1.2 s to reach the desired position) and there is no overshoot when reaching the reference. Also, the steady-state error is small, about 0.02 mm, which is a 0.1% of the total commanded displacement.

In the case of the incremental step reference (Fig. 7), the controller shows a performance very similar to the one of the previous test. There is an almost imperceptible overshoot in some of the ascending steps of the reference, but the overall behavior is good, with steady-state errors of about 5 μm, a 0.1% of the position increments.

5.2. PIPD

Figs. 8–10 show the results of the PIPD controller tracking the sinusoidal, step and incremental step references, respectively.

The controller exhibits noticeable oscillations around the reference during the ascending parts; the amplitude of the error is about 0.5 mm. These results are slightly worse than the ones obtained in [2], where this controller was first presented. These worse results are due to some differences between the experiments conducted in our previous work and the ones described here. In the first place, the SMA wires used in the cited work were shorter and with a smaller diameter, all of which result in a smaller thermal inertia. In addition, the hanging mass actuated by the SMA wire was lighter, which implies, among other things, that the transformation temperatures of the material were lower than in the present experiments. But the main reason lies on one of the disadvantages of the PIPD controller. Being a combination of two different controllers, one for the transient part of the actuation and the other one for the stationary part, different gains can be adjusted to obtain an optimal performance for each of these cases. That is, one set of gains can be used to optimize the behavior of the actuator for sinusoidal references, eminently transient, and a different set of gains can be tuned for step references, where the stationary behavior predominates. In
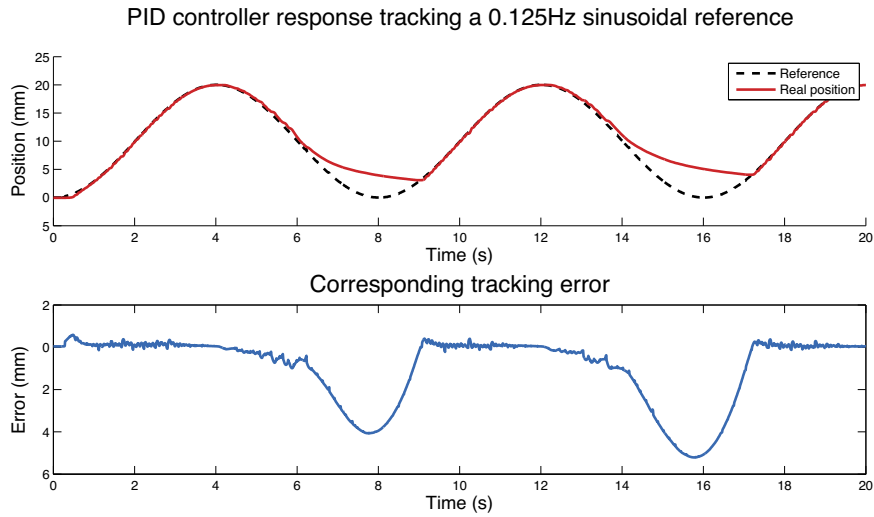
Fig. 5. Actuator position and error for the PID controller tracking a 0.125 Hz sinusoidal reference.
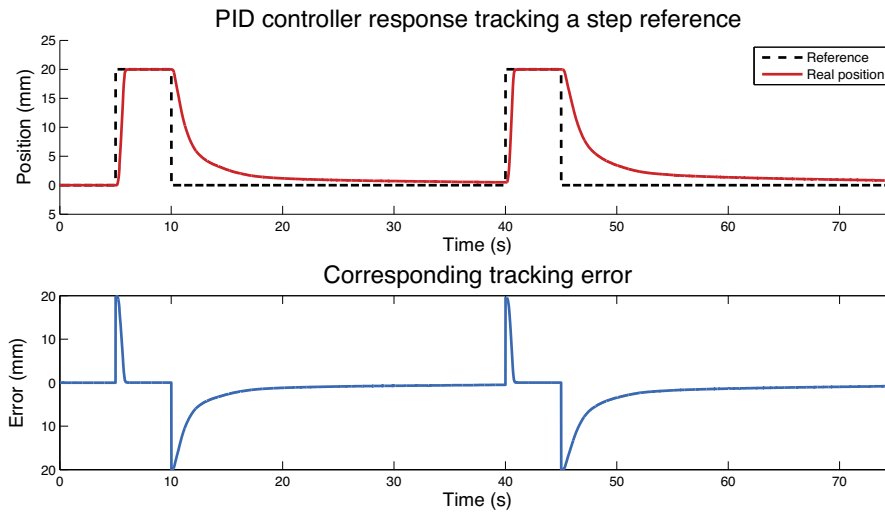

Fig. 6. Actuator position and error for the PID controller tracking a step reference.
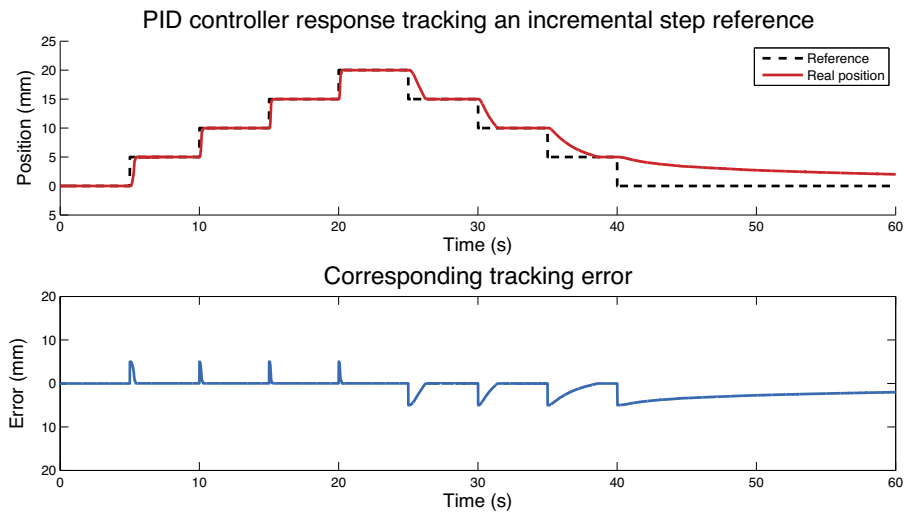

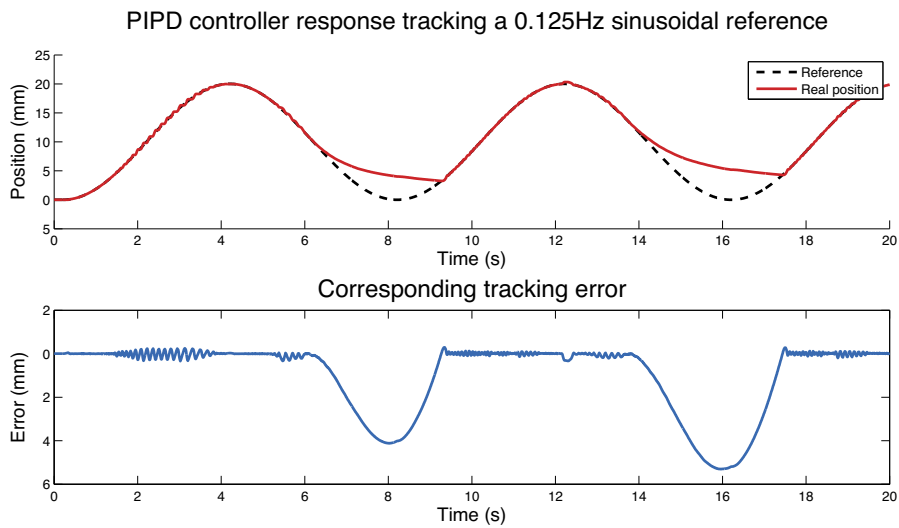**Fig. 7.** Actuator position and error for the PID controller tracking an incremental step reference.

Fig. 8. Actuator position and error for the PIPD controller tracking a 0.125 Hz sinusoidal reference.
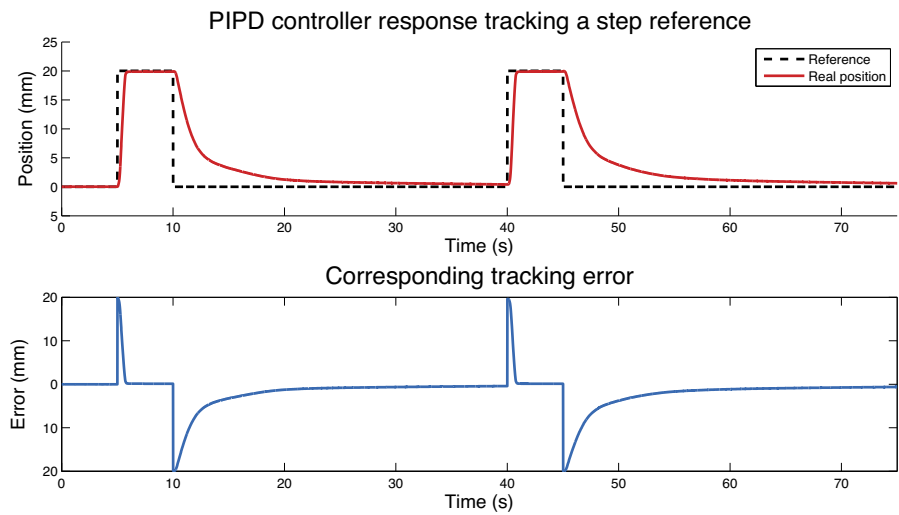

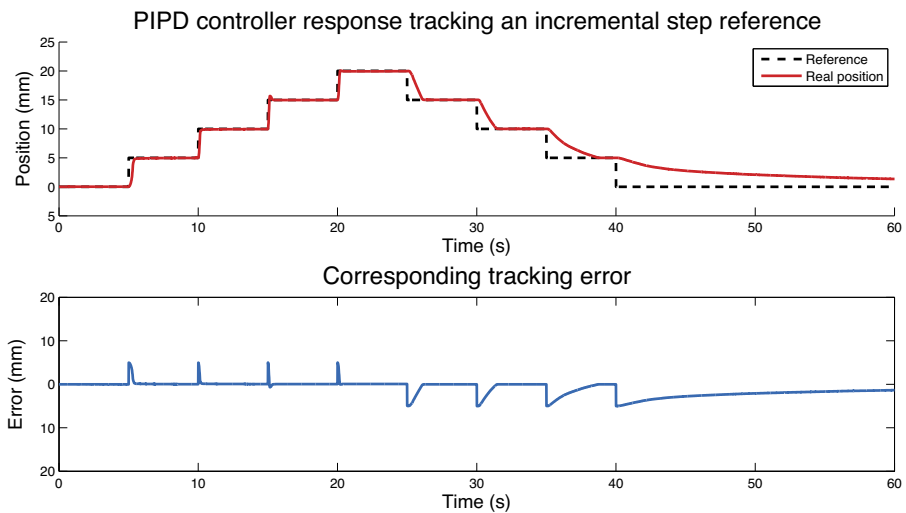**Fig. 9.** Actuator position and error for the PIPD controller tracking a step reference.

Fig. 10. Actuator position and error for the PIPD controller tracking an incremental step reference.
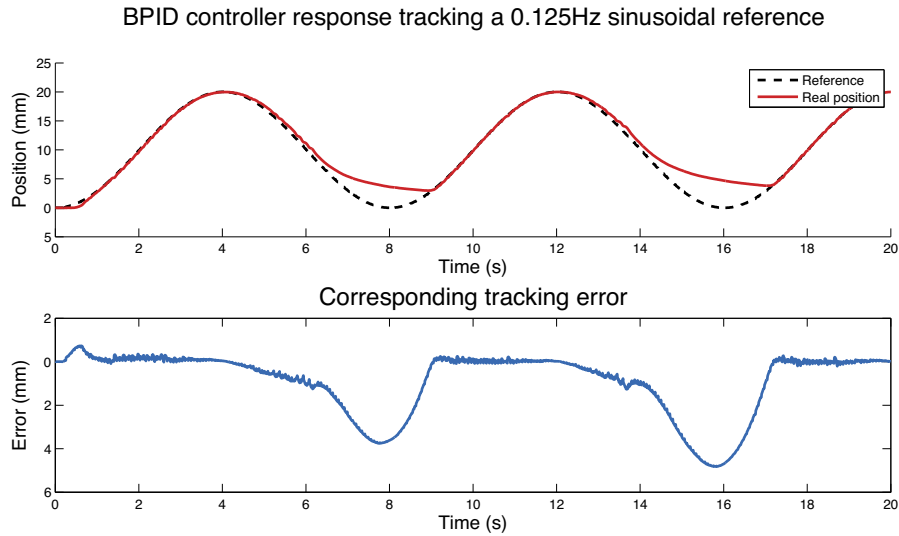
9

Fig. 11. Actuator position and error for the BPID controller tracking a 0.125 Hz sinusoidal reference.
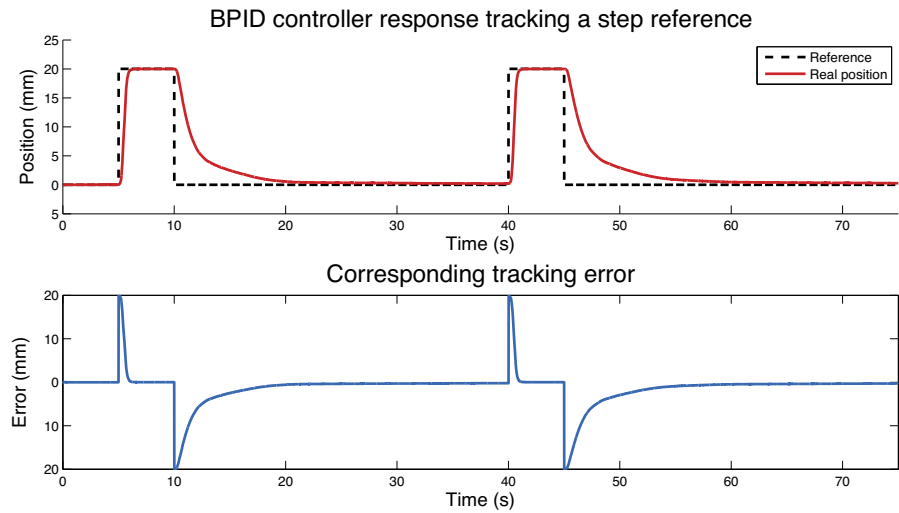

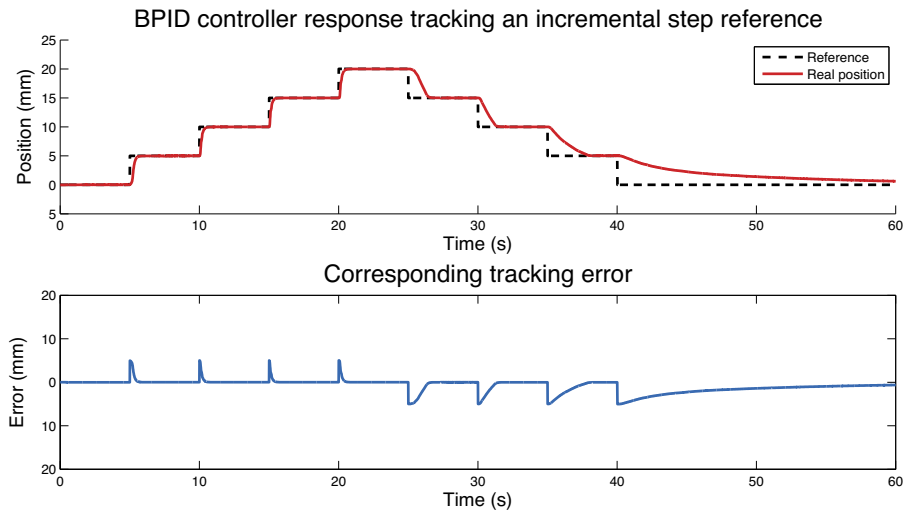**Fig. 12.** Actuator position and error for the BPID controller tracking a step reference.

Fig. 13. Actuator position and error for the BPID controller tracking an incremental step reference.

order not to give advantage to this controller over the other two during the tests, the same set of gains has been used for the five tests conducted. It is for this reason that the obtained results are not as good as the ones shown in our previous work.

The PIPD controller performs well on the step reference (Fig. 9). It shows no overshoot, despite the fact that its response is fast (1.1 s to reach the reference), and the steady-state error has a value of about 0.12 mm, which is a 0.6% of the total actuator displacement.

Tracking the incremental step reference (Fig. 10), the controlled actuator shows a similar behavior to the one obtained tracking the step reference. However, in this case there are some steps where there is overshoot, with an amplitude reaching a value of 0.7 mm (a 14% of the position variations). The steady-state error has a mean value of 0.05 mm, a 1% of the amplitude of the steps.

5.3. BPID

Figs. 11, 12 and 13 show the results of the BPID controller tracking the sinusoidal, step and incremental step references, respectively.

The behavior of the BPID controller tracking sinusoidal references is very similar to the one observed using the PID controller. The position of the actuator oscillates around the reference during the ascending parts, with an amplitude of 0.2 mm. Again, due to the thermal nature of the actuator, there is a final portion of the descending parts of the actuation cycle that the controller is not able to track.

It can be seen that the controller performs very well when tracking step references (Fig. 12), although it is the slowest of the three controllers, taking 1.4 s to reach the desired position. The response is very smooth when reaching the reference, with no overshoot. The steady-state error is about 0.02 mm, a 0.1% of the displacement.

With respect to the case of the controlled actuator tracking the incremental step reference (Fig. 13), the performance is very good. In fact, it is the best of the three controllers for this case. Unlike the PID and the PIPD controllers, the BPID shows no overshoot in any of the steps of the reference. The value of the steady-state error is about 0.01 mm, which is a 0.2% of the position increments.

5.4. Figures of merit

In this section, the different metrics used to quantitatively compare the performance of the three implemented controllers in the different tests carried out, will be shown in Tables 2–5. These metrics will help assessing if the proposed BPID controller has some advantages when compared with the other two tested controllers.

Table 2
Root mean squared error.

Reference type	0.125 Hz sine	0.250 Hz sine	0.500 Hz sine	Step	Incremental step
PID	1.71 mm	4.25 mm	7.66 mm	4.4 mm	1.96 mm
PIPD	1.95 mm	3.87 mm	6.5 mm	4.27 mm	1.75 mm
BPID	1.72 mm	3.51 mm	7.08 mm	4.1 mm	1.58 mm

Table 3
Integrated absolute value of the error.

Reference type	0.125 Hz sine	0.250 Hz sine	0.500 Hz sine	Step	Incremental step
PID	1.95×10^3 mm	5.85×10^3 mm	11.79×10^3 mm	1.81×10^4 mm	$7.33 * 10^3$ mm
PIPD	2.05×10^3 mm	5.01×10^3 mm	9.44×10^3 mm	1.62×10^4 mm	$6.41 * 10^3$ mm
BPID	2.06×10^3 mm	4.79×10^3 mm	10.72×10^3 mm	1.3×10^4 mm	$5.42 * 10^3$ mm

Table 4
Mean absolute control signal increment.

Reference type	0.125 Hz sine	0.250 Hz sine	0.500 Hz sine	Step	Incremental step
PID	14.13	8.81	6.24	0.71	1.92
PIPD	9.73	4.88	2.89	0.24	0.68
BPID	21.69	8.37	5.44	1.87	5.83

Table 5
Average power consumption.

Reference type	0.125 Hz sine	0.250 Hz sine	0.500 Hz sine	Step	Incremental step
PID	30.62 W	31.54 W	33.64 W	10.87 W	9.04 W
PIPD	25.23 W	29.83 W	32.04 W	10.56 W	8.23 W
BPID	32.56 W	33.62 W	35.41 W	11.46 W	10.99 W

5.4.1. Root mean squared error

RMSE is a very common value to assess the performance of a controller. It measures the square root of the average of the square of all the errors over the duration of the control test. Compared with the similar Mean Absolute Error, the RMSE amplifies and severely punishes large errors. The RMSE is computed as:

$$RMSE = \sqrt{\frac{1}{n}\sum_{i=1}^{n}[y_{ref}(i) - y(i)]^2} \tag{13}$$

5.4.2. Integrated absolute value of the error

The IAE gives a measure of the cumulative error over the duration of the control test. In this way, both large and small errors are taken into account. The IAE is computed as:

$$IAE = \int_{t=0}^{t=T}|y_{ref}(t) - y(t)|dt \tag{14}$$

5.4.3. Mean absolute control signal increment

The MACSI provides a measurement of how abrupt is the control signal that commutes the power of the SMA actuators. A more abrupt control signal (a control signal that has greater increments from one sample to the next) will impose greater variations of electrical power on the SMA actuator, which might shorten its service life. The MACSI is computed as:

$$MACSI = \frac{1}{n-1}\sum_{i=1}^{n-1}|u(i+1) - u(i)| \tag{15}$$

5.4.4. Average power consumption

The average power consumed by the actuator for each controller during the different tests has been measured. To compute it, the RMS value of the control signal (which is the duty cycle of a PWM signal) has been multiplied by the maximum squared current to

11

which the power supply of the SMA actuator has been limited ($4A$) and by the resistance of the SMA wire (4.2Ω):

$$AVPOW = \frac{\sqrt{\frac{1}{n}\sum_{i=1}^{n}u(i)^2}}{100} * I^2 * R_{SMA} \qquad (16)$$

6. Discussion

Once the results of every controller have been presented, the performance of every one must be analyzed in order to determine if the BPID controller is a viable alternative to control SMA actuators. In this section, the results of the three controllers are analyzed and compared. This comparative study will help to draw a conclusion on the validity of the control method proposed in this paper.

Regarding the sinusoidal references, the performance of each controller is very similar. However, the PIPD controller has a greater overshoot around the reference than the other two controllers, especially when tracking 0.125 Hz and 0.25 Hz sinusoidal signals. In contrast, this controller is able to track the reference during the descending part of the sine more accurately than the other two controllers (Fig. 14). The PID and BPID controllers have some delay at the start of the tests performed with the 0.25 Hz and 0.5 Hz references. In the three cases, the actuator is not able to track the final portion of the sinusoidal reference due to its cooling time, which is more noticeable in the case of the 0.5 Hz reference.

The RMSE and IAE values suggest that the BPID is slightly better than the other two controllers tracking sinusoidal references. The greatest difference is observed in the case of the 0.25 Hz reference, in which the BPID controller achieves the best performance. For the 0.5 Hz reference, the PIPD controller has better RMSE and IAE values than the PID and BPID because the latter follow the ascending part of the reference with some delay, whereas the greater response speed of the PIPD controller allows a more accurate tracking at this higher actuation frequency.

Comparing the results of the step reference, the performance of the three controllers is apparently the same, with no overshoot when reaching the reference. The steady-state error of the PID and BPID is practically the same, and smaller than the one of the PIPD. The fastest controller reaching the reference is the PIPD, although, during the descending part of the actuation, the BPID controller is faster than the other two, because it stops delivering power to the actuator earlier that the other two controllers. When looking at a detailed view of the ascending part of the actuation, some more differences can be seen (Fig. 15).

The response of the PIPD controller is faster than the other two controllers, reaching the reference earlier than the PID and the BPID. Due to the effect of the bilinear compensator, whose value becomes smaller as the position of the actuator approaches the reference, the speed of the SMA actuator when reaching the reference starts to decrease earlier than in the case of other two controllers, and it does so in a more gradual way. This effect of the bilinear term is very advantageous in cases like this, in which there is a sudden change of position, since it prevents overshoot.

With regard to the tests performed with the incremental step reference, the response of the three controllers is very similar. The BPID controller is again the fastest during the descending part of the actuation. A detailed view of the response of the controllers reveals more differences (Fig. 16).

The PIPD controller is the fastest of the three, but it has some overshoot (0.7 mm) when reaching the reference. The PID controller is faster than the BPID, although, just as in the previous test, the latter reaches the reference in a smoother and more regular way, preventing overshoot.

In relation to the RMSE values for these two tests, it can be said that the best performance is achieved by the BPID controller, followed by the PIPD and the PID controllers. Actually, although according to the RMSE values the PIPD controller performs better than the PID controller, by looking in detail at the response of the three controllers when tracking the step and the incremental step references, the PID controller performs slightly better that the PIPD controller, as can be seen in Fig. 16.

As with the RMSE, the measured IAE values imply that the best controller in terms of accuracy is the BPID, followed by the PIPD and the PID. But, as stated above, the PID controller is slightly better than the PIPD, especially when tracking step references. This can be seen in Fig. 17, which shows a detailed view of the actuator reaching the maximum step of the incremental step reference. Although both the PID and the PIPD controller overshoot when reaching the reference, the overshoot of the PID is smaller than the one of the PIPD. Also the steady-state error of the PID is smaller than the one of the PIPD, and also than the one of the BPID.

The overall performance of the PID controller is better than the performance of the PIPD controller, as shown in the previous figures. However, both the RMSE and IAE values, which measure the accuracy of the controllers, are bigger for the PID than for the PIPD. This contradiction could be explained by two reasons. First, the PIPD controller is the fastest of the three during the ascending part of the actuation, so its error while reaching the steady part of the reference has a shorter duration than the error of the other two
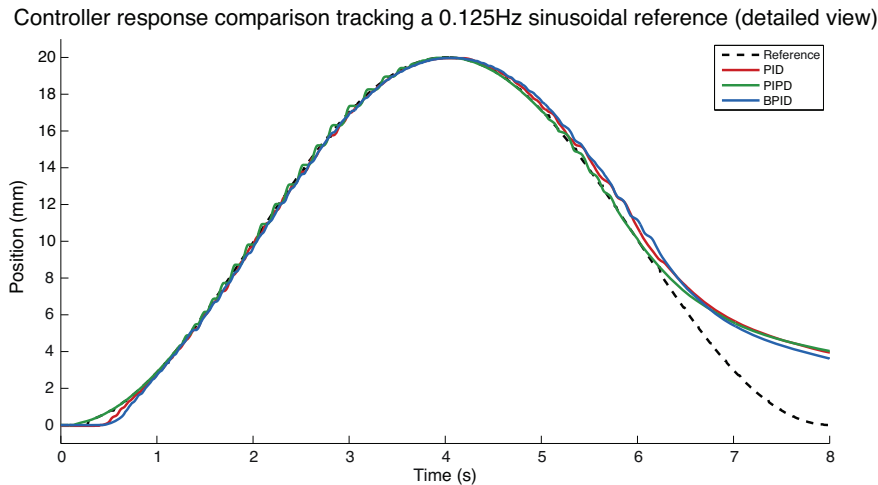

Fig. 14. Detailed view of the PID, PIPD and BPID tracking a 0.125 Hz sinusoidal reference.

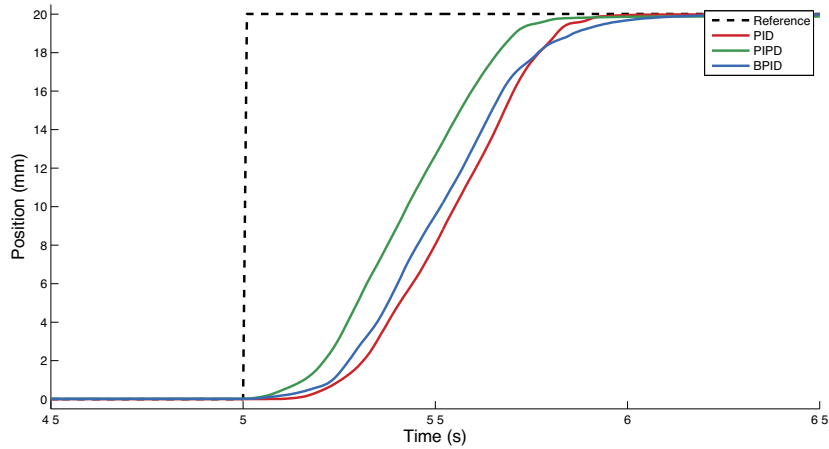Controller response comparison tracking a step reference (detailed view)

Fig. 15. Detailed view of the PID, PIPD and BPID tracking a step reference.

Controller response comparison tracking an incremental step reference (detailed view)
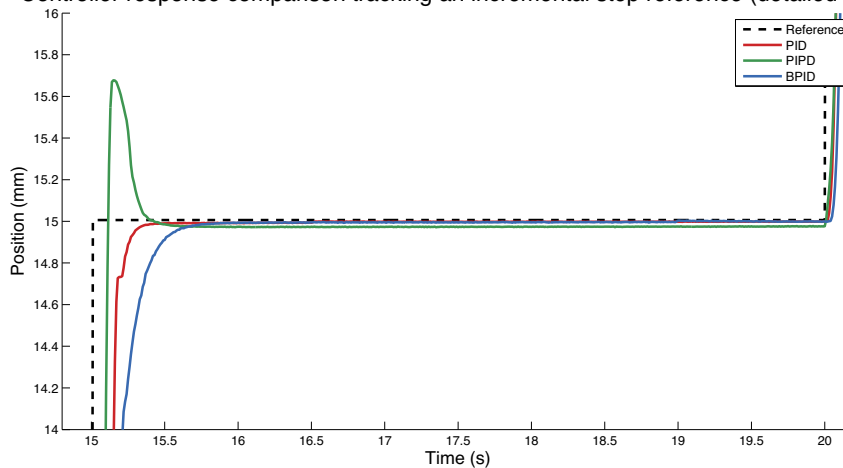

Fig. 16. Detailed view of the PID, PIPD and BPID tracking the third step of the incremental step reference.

controllers. This implies a smaller value of IAE, which accumulates error over time, for that portion of the actuation. The second reason has to do with the descending parts of the actuation. If we think of the IAE value as the area between the reference and the real position, it is clear from Fig. 18 that during the descending parts of the actuation, the PID controller has the greatest error, followed by the PIPD and the BPID controllers. This could explain why, although the performance of the PID controller is better than the one of the PIPD in the steady portions of the reference, the measured RMSE and IAE values are greater for this controller than for the PIPD.

As explained before, the MACSI value is a measurement of the "abruptness" of the control signal and therefore, a measurement of how large are the variations of the electrical power delivered to the SMA actuator. The amplitude of these energy fluctuations might affect the service life of the actuator. The processes of atomic rearrangement, which ultimately produce the shape memory effect, are triggered by a change in the temperature of the alloy, and this temperature variation is caused by the change of the electrical power fed into the SMA. The reorganization of the crystal structure of the material causes internal stresses that, after a number of transformation-recovery cycles, produce microcracks that start to degrade the alloy. Because of this, it might be assumed that if the control signal generated by the controller has great variations,

which result in large fluctuations of the input power of the actuator, the SMA would undergo greater partial phase transformations, that is, the crystal structure would be greatly modified, causing larger internal stresses and accelerating the appearance of microcracks which ultimately might lead to the breakage of the actuator.

From the MACSI measurements, it is clear that the controller that applies greater energy variations to the SMA actuator is the BPID, as can be seen in Fig. 19. The PIPD controller is the one of the three tested controllers which might increase the service life of the actuator. Still, the real effect of these differences on the abruptness of the control signal in the service life of the actuator should be studied to validate this hypothesis.

Finally, regarding power consumption, the average power consumed by the SMA actuator during each of the performed tests is very similar regardless of the selected controller. Both the PID and the BPID have a slightly greater power consumption when compared with the PIPD, which is consistent with their greater MACSI values.

An interesting conclusion can be drawn from the fact that the BPID controller has a slightly greater energy consumption than the other two controllers. The power consumption of the actuator is related to its input current, which is regulated by the controller output. Taking this into account, the slightly higher power consumption of the BPID controller means that it is more active than

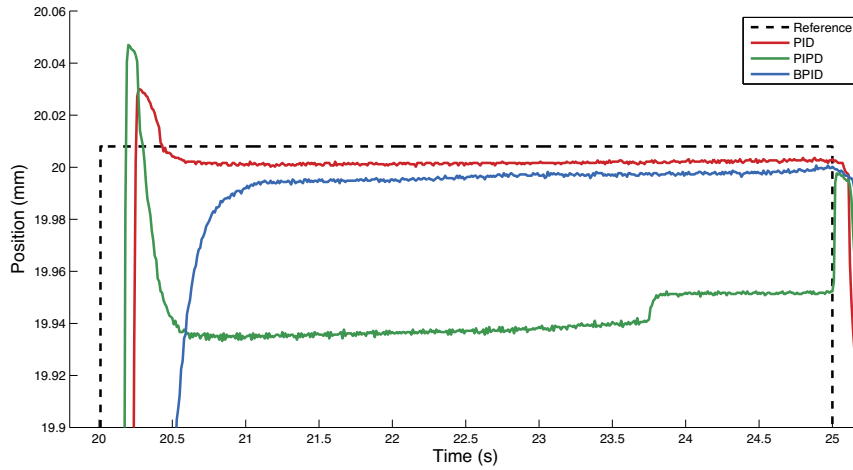Controller response comparison tracking an incremental step reference (detailed view)

Fig. 17. Detailed view of the PID, PIPD and BPID tracking the fourth step of the incremental step reference.

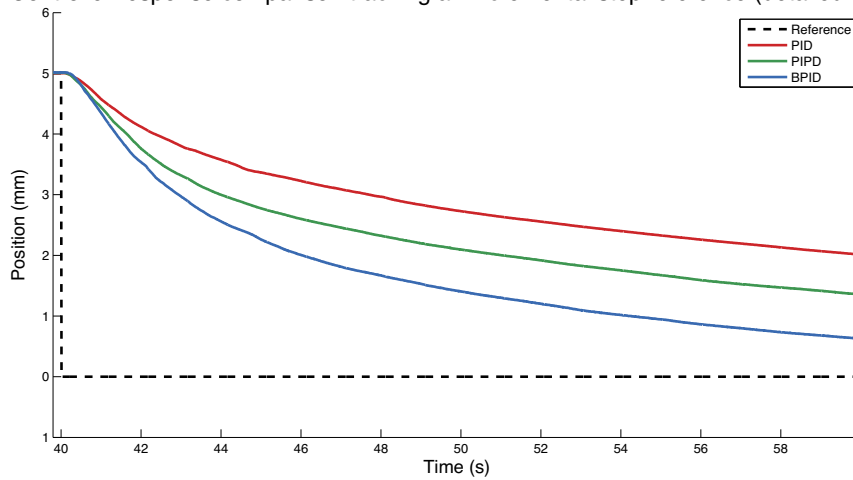Controller response comparison tracking an incremental step reference (detailed view)

Fig. 18. Detailed view of the PID, PIPD and BPID tracking the last portion of the incremental step reference.

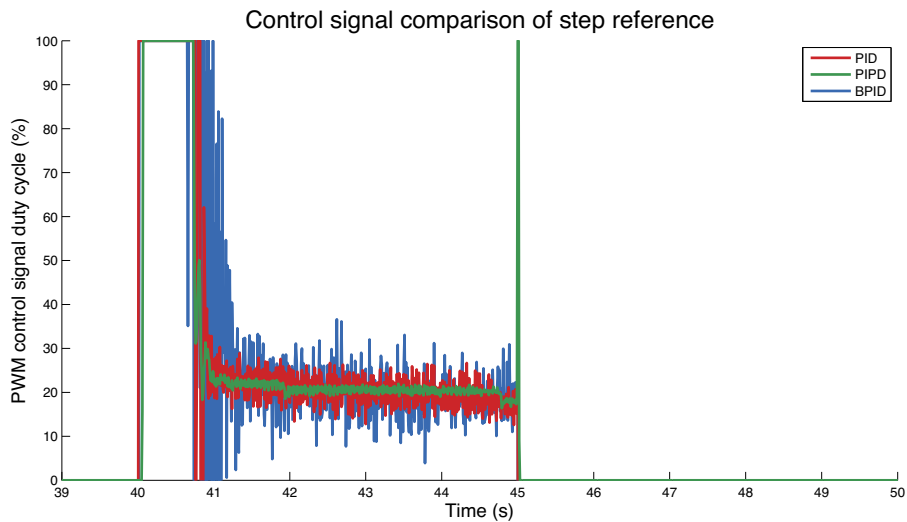Control signal comparison of step reference

Fig. 19. Control signal of the PID, PIPD and BPID tracking the first step of the step reference.

the other two controllers. The fact that the BPID controller is more active leads to the smoother actuator output with respect to the other two controllers.

7. Conclusions

In the light of the presented results, it can be stated that the BPID controller proposed in this work is a viable alternative to control the position of SMA actuators. As a SMA is a material with a nonlinear behavior, it is assumed that the most appropriate control techniques for those actuators based on this alloy are nonlinear controllers. Among the many existing controllers in the field of nonlinear control, we have considered bilinear controllers, and more specifically the four-term bilinear PID controller presented in this paper, as a promising alternative. Although there are many other options to control this kind of actuators with hysteresis, the bilinear controller that has been tested has the advantage of being simpler to implement than control strategies such as inverse hysteresis model controllers that, besides having a greater complexity, require the application of a series of model identification techniques which extend the implementation process and make the controller operate optimally only under those conditions in which the actuator has been identified. Because the bilinear term linearizes the dynamic behavior of the plant, the well known analytical techniques existing for linear systems can be applied to this type of nonlinear controller.

The conducted tests and the different metrics that have been computed from these tests allow to draw some conclusions. When subjected to sinusoidal references, there is little difference between the three strategies. At low actuation frequencies, the PID and BPID controllers perform better than the PIPD, which oscillates noticeably around the reference during its ascending portions. However, the latter controller performs better than the former ones during the descending parts of the reference. Also, at the highest tested frequency, 0.5 Hz, the performance of the PIPD controller is better than the one of the other two. The behavior of the PID and BPID controllers is very similar at low frequencies, but as the actuation frequency increases, the results obtained with the BPID improve with respect to the ones obtained with the PID strategy.

The greatest differences in the performance of the three controllers have been observed in the experiments in which the actuator tracks step references, both for great position variations and for small position increments. In none of the many tests performed, the BPID controller has produced overshoot, unlike the other two tested controllers. This is because of the gain introduced by the bilinear compensator, which increases the control action when the position of the actuator is far from the reference, and decreases it as the actuator approaches the commanded position. For step references, the only disadvantage of the bilinear term is that it slightly reduces the speed of the controller, but compared with the PID and PIPD strategies, the difference is only 0.2 s and 0.3 s, respectively.

One of the downsides of the BPID controller is that, among the three tested controllers, it is the one which produces the greatest variations in the input power of the actuator, which might affect its service life. The MACSI value of the BPID controller is the greatest of the three controllers in all the performed experiments. As defined above, the MACSI value measures the amplitude of the variations of the control signal which are directly related to the fluctuations of the electrical power delivered to the SMA actuator. It might be assumed that the higher the variations of the input power, the shorter the service life of the actuator, since the thermal cycles to which it is subjected have a greater temperature difference, which entails a bigger change in the martensite fraction of the material, that is, a greater change in the crystal structure of the material, that eventually would lead to the emergence of

microcracks that would permanently damage the actuator. From the computed MACSI values that measure the mean amplitude of the control signal increments, it can be concluded that, if the above hypothesis is correct, the controller that would increase the service life of the actuator is the PIPD. Still, it has to be assessed to what extent the fluctuations of the control signal have an impact on the service life of the SMA actuator.

Although the SMA actuator has a slightly greater power consumption and its service life might be shorter when controlled with the BPID strategy, regarding its accuracy when tracking a given position reference, the BPID controller outperforms the other two tested strategies. Further experiments have to be conducted to study how the use of different gains in the bilinear compensator affects the performance of the controller, since one of the alleged advantages of the BPID strategy is that the bilinear compensator allows increasing the PID gains to improve the speed of the controller without degrading its performance. Also, the proposed control strategy should be compared with other nonlinear control techniques.

References

[1] Technical Characteristics of Flexinol Actuator Wires, DYNALLOY, Inc., 2014.
[2] A. Flores, D. Copaci, A. Martín, D. Blanco, L. Moreno, Smooth and accurate control of multiple shape memory alloys based actuators via low cost embedded hardware, in: Workshop on Smart Materials and Alternative Techonologies for Bio-inspired Robots and Systems at: IEEE/RSJ International Conference on Intelligent Robots and Systems, IROS, 2012.
[3] C. Bruni, G. Dipillo, G. Koch, Bilinear systems: an appealing class of nearly linear systems in theory and applications, IEEE Trans. Autom. Control 19 (1974) 334–348.
[4] H.J. Lee, J.J. Lee, Time delay control of a shape memory alloy actuator, Smart Mater. Struct. 13 (2004) 227–239.
[5] H. Sayyaadi, M.R. Zakerzadeh, Position control of shape memory alloy actuator based on the generalized Prandtl–Ishlinski inverse model, Mechatronics 22 (2012) 945–957.
[6] E.P. Da Silva, Beam shape feedback control by means of a shape memory actuator, Mater. Des. 28 (2007) 1592–1596.
[7] E. Shameli, A. Alasty, H. Salaarieh, Stability analysis and nonlinear control of a miniature shape memory alloy actuator for precise applications, Mechatronics 15 (2005) 471–486.
[8] S.M. Yang, J.H. Roh, J.H. Han, I. Lee, Experimental studies on active shape control of composite structures using SMA actuators, J. Intell. Mater. Syst. Struct. 17 (2006) 767–777.
[9] A.V. Popov, M. Labib, J. Fays, R.M. Botez, Closed-loop control simulations on a morphing wing, J. Aircr. 45 (2008) 1794–1803.
[10] E. Asua, V. Etxebarria, A. García-Arribas, Micropositioning control using shape memory alloys, in: Control Applications, 2006. CCA 2006. Proceedings of 2006 IEEE Conference on, Munich, Germany, 2006, pp. 3229–3234.
[11] N. Ma, G. Song, Control of shape memory alloy actuator using pulse width modulation, Smart Mater. Struct. 12 (2003) 712–719.
[12] G. Song, N. Ma, Control of shape memory alloy actuators using pulse-width pulse-frequency (PWPF), J. Intell. Mater. Syst. Struct. 14 (2003) 15–22.
[13] K.K. Leang, S. Ashley, G. Tchoupo, Iterative and feedback control for hysteresis compensation in SMA, J. Dyn. Syst. Meas. Control 131 (2009), 014502-1–014502-6.
[14] A. Kumagi, T.I. Liu, P. Hozian, Control of shape memory alloy actuators with a neuro-fuzzy feedforward model element, J. Intell. Manuf. 17 (2006) 45–56.
[15] G. Song, V. Chaudhry, C. Batur, A neural network inverse model for a shape memory alloy wire actuator, J. Intell. Mater. Syst. Struct. 14 (2003) 371–377.
[16] A. Rezaeeian, A.Y. Koma, B. Shasti, A. Doosthoseini, ANFIS modeling and feedforward control of shape memory alloy actuators, in: Proceedings of the 10th

WSEAS International Conference on Automatic Control, Modelling & Simulation, 2008. ACMOS'08, 2008, pp. 243–248.

[17] S. Majima, K. Kodama, T. Hasegawa, Modeling of shape memory alloy actuator and tracking control system with the model, IEEE Trans. Control Syst. Technol. 9 (2001) 54–59.

[18] C.H. Lee, C. Mavroidis, Analytical dynamic model and experimental robust and optimal control of shape-memory-alloy bundle actuators, in: ASME 2002 International Mechanical Engineering Congress and Exposition, 2002, pp. 491–498.

[19] J. Jayender, R.V. Patel, S. Nikumb, M. Ostojic, Modelling and gain scheduled control of shape memory alloy actuators, in: Proceedings of 2005 IEEE Conference on Control Applications, 2005. CCA 2005, 2005, pp. 767–772.

[20] J. Jayender, R.V. Patel, S. Nikumb, M. Ostojic, Modeling and control of shape memory alloy actuators, IEEE Trans. Control Syst. Technol. 16 (2008) 279–287.

[21] A. Kilicarslan, K. Grigoriadis, G. Song, Compensation of hysteresis in a shape memory alloy wire system using linear parameter-varying gain scheduling control, IET Control Theory Appl. 8 (2014) 1875–1885.

[22] K. Andrianesis, Y. Koveos, G. Nikolakopoulos, A. Tzes, Shape Memory Alloys, Sciyo, 2010, pp. 81–106.

[23] L.C. Brinson, M.S. Huang, Simplifications and comparisons of shape memory alloy constitutive models, J. Intell. Mater. Syst. Struct. 7 (1996) 108–114.

[24] H. Ashrafiuon, V.R. Jala, Sliding mode control of mechanical systems actuated by shape memory alloy, J. Dyn. Syst. Meas. Control 131 (2009), 011010-1–011010-6.

[25] M. Elahinia, Effect of System Dynamics on Shape Memory Alloy Behavior and Control, Virginia Polytechnic Institute and State University, Blacksburg, Virginia, USA, 2004 (Ph.D. thesis).

[26] M.H. Elahinia, M. Ahmadian, Application of the extended Kalman filter to control of a shape memory alloy arm, Smart Mater. Struct. 15 (2006) 1370–1384.

[27] W.S. Galinaitis, Two methods for modeling scalar hysteresis and their use in controlling actuators with hysteresis, Virginia Polytechnic Institute and State University, Blacksburg, Virginia, USA, 1999 (Ph.D. thesis).

[28] C. Ru, L. Chen, B. Shao, W. Rong, L.W. Sun, A hysteresis compensation method of piezoelectric actuator: model, identification and control, Control Eng. Pract. 17 (2009) 1107–1114.

[29] D. Hughes, J. Wen, Preisach modeling and compensation for smart material hysteresis, in: Proceedings of SPIE on Active Materials and Smart Structures, vol. 2427, 1995, pp. 50–64.

[30] K.K. Ahn, N.B. Kha, Improvement of the performance of hysteresis compensation in SMA actuators by using inverse Preisach model in closed-loop control system, J. Mech. Sci. Technol. 20 (2006) 634–642.

[31] G.V. Webb, D.C. Lagoudas, A.J. Kurdila, Hysteresis modeling of SMA actuators for control applications, J. Intell. Mater. Syst. Struct. 9 (1998) 432–448.

[32] R.R. Mohler, R.E. Rink, Control with a multiplicative model, ASME J. Basic Eng. 91 (1969) 201–205.

[33] R.E. Rink, R. Mohler, Completely controllable bilinear systems, SIAM J. Control 6 (1968) 477–486.

[34] J.A. Minihan, Design of bilinear controllers for industrial plants, Coventry University, Coventry, UK, 2001 (Ph.D. thesis).

[35] S. Martineau, K.J. Burnham, O.C.L. Haas, G. Andrews, A. Heeley, Four-term bilinear PID controller applied to an industrial furnace, Control Eng. Pract. 12 (2004) 457–464.

[36] A. Villoslada, A. Flores, D. Copaci, D. Blanco, L. Moreno, High-displacement flexible shape memory alloy actuator for soft wearable robots, Robot. Auton. Syst. 73 (2015) 91–101.

[37] A. Villoslada, A. Flores, D. Copaci, D. Blanco, L. Moreno, High-displacement fast-cooling flexible shape memory alloy actuator: application to an anthropomorphic robotic hand, in: 2014 14th IEEE-RAS International Conference on Humanoid Robots (Humanoids), 2014, pp. 27–32.

[38] F. Butera, M. Biasiotto, S. Alacqua, Actuator device with a flexible cable incorporating a shape-memory element, 2004.

[39] R. Neugebauer, K. Pagel, A. Bucht, W.G. Drossel, Model-based position control of shape memory alloy actuators, Int. J. Mech. Manuf. Syst. 5 (2012) 93–105.

[40] A. Flores, Sistema avanzado de prototipado rápido para control en exoesqueletos y dispositivos mecatrónicos, Universidad Carlos III de Madrid, 2015 (Ph.D. thesis).

Biographies

Álvaro Villoslada obtained his B.Sc. degree in Electronics Engineering from the Carlos III University of Madrid, Spain, in the year 2010. In 2012, he received his M.Sc. degree in Robotics and Automation from the same university. His M.Sc. Thesis, entitled "Design and implementation of a myoelectric control system for a printable robotic hand", was awarded with the VI Treelogic Award to the Innovative Spirit. In the present day he is a Ph.D. student working as a Research Assistant in the STAMAS Project (EU FP7 Project). His current research is focused in the design, modeling and control of SMA actuators for actuated space suit gloves.

Naiara Escudero received the B.Sc. degree in Telecommunication Engineering from the Carlos III University of Madrid, Spain, in 2013, and the Master's degree in Robotics and Automation also from the Carlos III University of Madrid in 2015. In 2012, she started her professional career at Arquimea Ingeniería. Her work is focused on robotic control systems and smart materials control.

Fernando Martín received the Degree in Industrial Engineering in 2005 from the Carlos III University of Madrid, Spain, and the Ph.D. degree in 2012 from the same university. In 2006, he joined the Department of Systems Engineering and Automation, Carlos III University of Madrid, where he has been involved in several mobile robotics projects. His research interests are in the areas of control engineering, nonlinear systems, mobile robotics, mobile manipulators, 3D environment modeling, evolutionary computation, and mobile robot global localization problems.

Antonio Flores obtained his degree in Electronics Engineering from the Carlos III University of Madrid, Spain, in 2008. He obtained his M.Sc. degree in Robotics and Automation from the Carlos III University of Madrid in 2011, and the Ph.D. degree in 2015 from the same university. His work is focused on the development of custom control hardware and software, and on the development of custom Simulink toolboxes to develop rapid control prototyping systems.

Cayetano Rivera received the Degree in Industrial Engineering in 2012 from the Carlos III University of Madrid, Spain. In 2011 he joined the R&D department of Arquímea Ingeniería where he has been involved in several projects in fields such as mechanical design of Space actuators, biomechanic devices such as implants and exoskeletons, and others.

Marcelo Collado obtained his B.Sc. degree in Telecommunication Engineering: Telecommunication Systems and Networks from the Carlos III University of Madrid in the year 2008. In 2012, he completed his M. Sc. degree in Space and Satellite Technology at Polytechnic University of Madrid. Since 2007 he has been working for Arquimea Ingeniería, being involved in several R&D programs in different disciplines, mainly for aerospace applications. Currently, he is leading the Smart Materials group and is the Project Coordinator in the STAMAS Project (EU FP7). His main research is focused in the area of shape memory alloys, both in the development, processing, characterization and application of novel alloys and the design, modeling and control of SMA actuators.

Professor Luis Moreno received the Degree in Automation and Electronics Engineering in 1984 and the Ph.D. degree in 1988 from the Polytechnic University of Madrid, Spain. From 1988 to 1994, he was an associate professor at the Polytechnic University of Madrid. In 1994, he joined the Systems Engineering and Automation Department at Carlos III University of Madrid, Spain, where he has been involved in several mobile robotics projects. His research interests are in the areas of control, mobile robotics, mobile manipulators, environment modeling, path planning and mobile robot global localization problems.